J. Fluid Mech. (1976), *vol.* 76, *part* 3, *pp.* 481–499
Printed in Great Britain

Convection due to internal heat sources

By MORTEN TVEITEREID AND ENOK PALM
Department of Mechanics, University of Oslo, Norway

(Received 19 June 1975 and in revised form 15 March 1976)

This paper is concerned with convection generated by uniformly distributed internal heat sources. By a numerical method it is found that the planform is down-hexagons for infinite Prandtl numbers and Rayleigh numbers up to at least 15 times the critical value. The motion is also studied for finite Prandtl numbers and small supercritical Rayleigh numbers by using an amplitude expansion. It turns out that a small subcritical regime exists. Moreover, it also emerges that for Prandtl numbers less than 0·25 the stable planform is up-hexagons. In §3 a necessary condition in order to obtain a hexagonal planform is derived when the coefficients in the differential equations are a function of the vertical co-ordinate z.

1. Introduction

The purpose of this paper is to examine thermal convection generated by internal heat sources. This problem arises in connexion with the study of convection in the earth's mantle, where the heat sources are due to radioactive material. The problem may also have a bearing on the thermal convection in clouds. This kind of convection is, however, very complicated since the heat sources, being released latent heat, depend strongly on the vertical motion.

Convection by internal heat sources has been studied in several papers. Closely related to the present paper are the experimental studies by Tritton & Zarraga (1967) and Schwiderski & Schwab (1971) and the theoretical studies by Roberts (1967) and Thirlby (1970). Other papers on convection with internal heat sources have been published by Sparrow, Goldstein & Jonsson (1964), Whitehead & Chen (1970), Kulacki & Goldstein (1972) and McKenzie, Roberts & Weiss (1974). It is found that the motion is dependent on two dimensionless parameters: the Rayleigh number R (in a modified form) and the Prandtl number P. It is also found in the theory that for small Rayleigh numbers the heat is transported by conduction alone. For Rayleigh numbers larger than a certain value R_0, dependent on the horizontal wavenumber a, but independent of the Prandtl number, heat transfer also takes place by convection. The minimum value of R_0 will be called R_c and the corresponding value of the wavenumber a_c. No experiments have to our knowledge been performed in which the computed values of R_c and a_c have been tested.

The experiments by Tritton & Zarraga and Schwiderski & Schwab are confined to higher Rayleigh numbers, from $4R_c$ up to about $80R_c$. The main result of

these experiments is that a marked tendency towards formation of a hexagon-like pattern exists for Rayleigh numbers up to about $40R_c$. For still higher R the hexagonal planform seems to be replaced by more 'roll-like' cells. The horizontal wavenumbers of the hexagons are close to a_c for Rayleigh numbers of about $4R_c$. Above this value the horizontal length scale increases markedly. This observation may, however, be due to some unwanted imperfections in the experiments, a point we shall return to in §7. The convective fluid in the experiments was aqueous zinc sulphate solution with a Prandtl number of about 5·5. It was found for this fluid that the hexagons were down-hexagons, i.e. descending flow occurred in the centres of the cells and ascending flow at their peripheries. These findings resemble the results for ordinary Bénard convection when the fluid possesses a viscosity increasing with temperature. The essential difference is that the interval containing hexagons is much larger in the present case (see Palm 1975). A similar pattern of hexagons was found by Krishnamurti (1968*a*, *b*) when examining convection in a fluid with a time-dependent mean temperature. The convection set up in her experiment may in fact be interpreted as convection generated by internal heat sources. The main difference between the present problem and Krishnamurti's is that in the latter case the effect of the heat sources is added to the ordinary Bénard convection as a perturbation.

Roberts based his theory on a kind of mean-field approximation. This approximation reduces effectively the computational work necessary and has been applied with great success to obtain the relation between the Nusselt number and the Rayleigh number for high Rayleigh numbers (Herring 1963, 1964). Roberts applied this method to study the stability of the steady nonlinear solutions. He found that for $P = 6{\cdot}7$ the stable hexagons are down-hexagons, in agreement with observation. He also found, however, that no steady hexagons exist for $R < 3R_c$ and that two-dimensional rolls are stable for all R. There are no experiments available to check this result. On the other hand, this is in disagreement with the result found in the present paper by an amplitude expansion. It is also in disagreement with our numerical results for infinite Prandtl number. This discrepancy may be due to the method he applied, which is probably too crude for this purpose.

Thirlby computed the stability of the motion by applying a finite-difference method. He too obtained stable down-hexagons for a similar Prandtl number. He found, however, that hexagons only exist for R larger than about $5R_c$, whereas for $R_c < R < 5R_c$ a kind of rectangular cell pattern is stable. This result disagrees with our findings since we find that hexagons are the only stable planform for small supercritical Rayleigh numbers. For infinite Prandtl number we find that the hexagons are stable for values of R at least up to 15 times the critical value.

In §2 we shall derive the governing equations. In §3 we shall derive a condition concerning the possibility of obtaining a hexagonal planform when the fluid properties depend explicitly on the vertical co-ordinate z (instead of explicitly on the temperature). In §4 the steady solutions for infinite Prandtl number are derived by a numerical technique. The stability of these solutions is examined in §5. In §6 we apply an amplitude expansion, partly to examine the possibility

of subcritical instability and partly to study the convection for various Prandtl numbers. One result of this expansion procedure is that for Prandtl numbers lower than about 0·25 up-hexagons are found to be stable.

2. The governing equations

We consider a fluid layer of constant depth d and of infinite horizontal extent. To be in agreement with the experimental conditions, we assume that heat is generated uniformly in the fluid. Furthermore, the fluid is supposed to be bounded above by a rigid perfectly conducting plane maintained at constant temperature and to be bounded below by a rigid insulating plane.

In the Boussinesq approximation the basic equations become

$$\partial \mathbf{v}/\partial t + \mathbf{v}.\nabla \mathbf{v} = \rho_0^{-1}\nabla p - [1-\alpha(T-T_0)]\,g\mathbf{k} + \nu\nabla^2\mathbf{v}, \tag{2.1}$$

$$\nabla.\mathbf{v} = 0, \tag{2.2}$$

$$\partial T/\partial t + \mathbf{v}.\nabla T = \kappa\nabla^2 T + Q/\rho_0 c_p, \tag{2.3}$$

with the boundary conditions

$$\left.\begin{aligned} &\mathbf{v} = 0, \quad \partial T/\partial z = 0 \quad \text{at} \quad z = 0, \\ &\mathbf{v} = 0, \quad T = 0 \qquad \text{at} \quad z = d. \end{aligned}\right\} \tag{2.4}$$

Here t denotes the time, $\mathbf{v}(u, v, w)$ the velocity, p the pressure, T the temperature, T_0 a reference temperature, ρ_0 a reference density, Q the (constant) amount of heat generated per unit time and unit volume, g the acceleration due to gravity, $\mathbf{k}$ a unit vector directed upwards, z the vertical co-ordinate, α the coefficient of expansion, ν the kinematic viscosity, κ the thermal diffusivity and c_p the specific heat.

If the heat generated Q is sufficiently small, the heat transfer will be in the form of conduction. A steady-state flow then exists where

$$T = T_s(z) = (Q/2\kappa\rho_0 c_p)\,(d^2 - z^2), \quad p = p_s(z), \quad \mathbf{v} = 0. \tag{2.5}$$

For larger values of Q, in the convective regime, we write

$$T = T_s + \theta(x, y, z, t), \quad p = p_s + p'(x, y, z, t). \tag{2.6}$$

The equations may be non-dimensionalized by using d, d^2/κ, κ/d, $\kappa\nu\rho_0/d^2$ and $\kappa\nu/g\alpha d^3$ as units of length, time, velocity, pressure and temperature, respectively. Omitting the prime in the pressure term, the equations then take the form

$$P^{-1}(\partial \mathbf{v}/\partial t + \mathbf{v}.\nabla \mathbf{v}) = -\nabla p + \theta\mathbf{k} + \nabla^2\mathbf{v}, \tag{2.7}$$

$$\nabla.\mathbf{v} = 0, \tag{2.8}$$

$$\partial T/\partial t + \mathbf{v}.\nabla\theta = \nabla^2\theta + Rzw, \tag{2.9}$$

with the boundary conditions

$$\left.\begin{aligned} &\mathbf{v} = \partial\theta/\partial z = 0 \quad \text{at} \quad z = 0, \\ &\mathbf{v} = \theta = 0 \qquad \text{at} \quad z = 1. \end{aligned}\right\} \tag{2.10}$$

Here P is the Prandtl number and R the modified Rayleigh number, defined by

$$P = \nu/\kappa, \quad R = g\alpha Q d^5/\kappa^2 \nu \rho_0 c_p. \tag{2.11}$$

By means of (2.7)–(2.10) we shall obtain a set of steady-state solutions. To investigate which of these are stable we introduce an infinitesimal perturbation $(\tilde{\mathbf{v}}, \tilde{\theta}, \tilde{p})$ with a time dependence of the form $\exp(\sigma t)$. The perturbation equations may then be written as

$$P^{-1}(\sigma\tilde{\mathbf{v}} + \mathbf{v}.\nabla\tilde{\mathbf{v}} + \tilde{\mathbf{v}}.\nabla\mathbf{v}) = -\nabla\tilde{p} + \tilde{\theta}\mathbf{k} + \nabla^2\tilde{\mathbf{v}}, \tag{2.12}$$

$$\nabla.\tilde{\mathbf{v}} = 0, \tag{2.13}$$

$$\sigma\tilde{\theta} + \mathbf{v}.\nabla\tilde{\theta} + \tilde{\mathbf{v}}.\nabla\theta = \nabla^2\tilde{\theta} + Rz\tilde{w}, \tag{2.14}$$

with the boundary conditions

$$\left.\begin{aligned} &\tilde{\mathbf{v}} = \partial\tilde{\theta}/\partial z = 0 \quad \text{at} \quad z = 0, \\ &\tilde{\mathbf{v}} = \tilde{\theta} = 0 \qquad \text{at} \quad z = 1. \end{aligned}\right\} \tag{2.15}$$

For known values of $\mathbf{v}$ and θ these equations pose an eigenvalue problem for σ, determining the stability behaviour of the steady solution.

The Rayleigh number R_0 at the onset of convection may be found from the linearized version of (2.7)–(2.10). Introducing the horizontal wavenumber a, defined by

$$\partial^2/\partial x^2 + \partial^2/\partial y^2 = -a^2, \tag{2.16}$$

R_0 becomes a function of a. This function is most readily found by developing the solution in a power series in z, as proposed by Sparrow *et al.* (1964). The result is shown in figure 1. The minimum value R_c of R_0 and the corresponding value a_c of a are found to be

$$R_c = 2772{\cdot}27, \quad a_c = 2{\cdot}63, \tag{2.17}$$

which are identical to the values found by Roberts.

3. The occurrence of hexagonal patterns

Compared with the equation for ordinary Bénard convection, the system of equations (2.7)–(2.10) is distinguished by one of the coefficients being a function of z. As mentioned in § 1, such a system of equations is also obtained in the transient problem. It is obtained too when some fluid property depends explicitly on z. Thus, by choosing the thermal diffusivity as a suitable function of z, we obtain governing equations which are formally the same as (2.7)–(2.10). Fluid properties varying with z may occur in thermal convection in a porous layer with varying grain diameter. A z-dependent (turbulent) viscosity or conductivity may also occur in convection in a turbulent fluid, for example in clouds.

It is well established in the theory of Bénard convection that, for fluids with properties depending on the temperature, the planform will be hexagons at least for values of R close to R_c (Palm 1960; Busse 1962). The question arises as to whether this is true also when the fluid properties are functions of z explicitly. If the answer is in the affirmative, we may conclude that this planform will occur also in the present case.

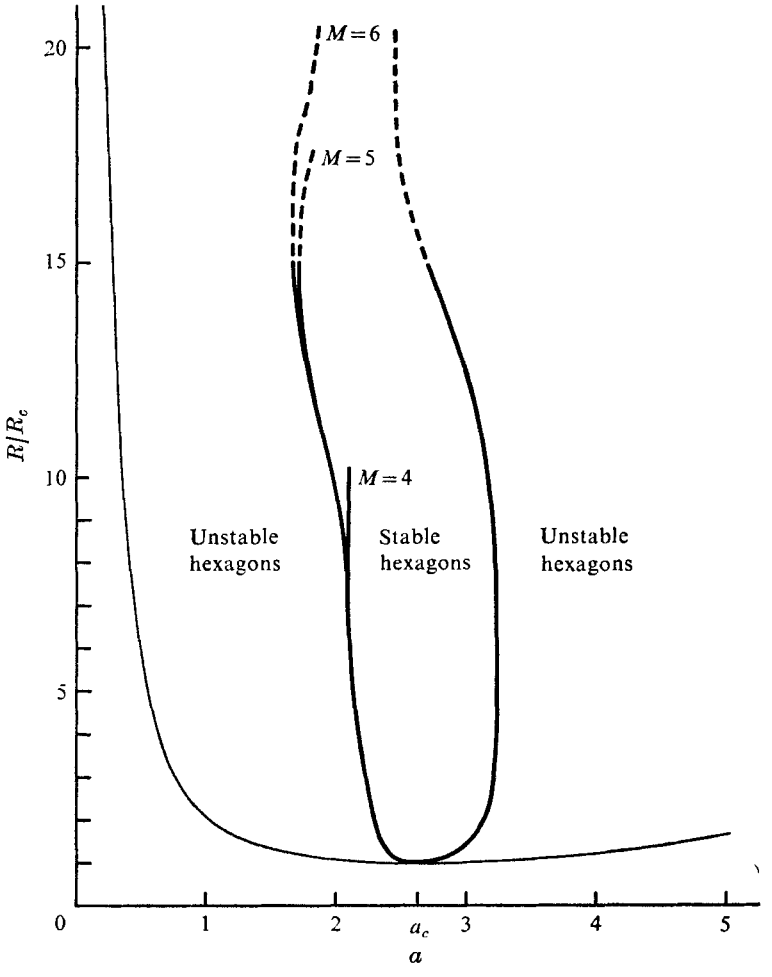

FIGURE 1. The region of stability for hexagons. This figure is based on calculated values for the Rayleigh numbers R_c = 2772, 3000, 3200, 3500, 4000, 4500, 5000, $2R_c$, $2{\cdot}5R_c$, ..., $5R_c$, $6R_c$, ..., $10R_c$, $12R_c$, $14R_c$, $15R_c$, $18R_c$, $20R_c$.

We shall consider Rayleigh numbers close to R_c and write

$$R - R_0 = \Delta R = R_1 + R_2 + \ldots, \tag{3.1}$$

where R_1 is of first order in the amplitude, R_2 of second order and so on. We introduce for the moment the four-dimensional vector $\mathbf{u} = (\mathbf{v}, \theta)$, which correspondingly may be written as

$$\mathbf{u} = \mathbf{u}_1 + \mathbf{u}_2 + \ldots . \tag{3.2}$$

From the amplitude expansion in Palm (1960), Busse (1962) or Palm, Ellingsen & Gjevik (1967) it follows that it is the term R_1 in (3.1) (equivalent to the second-order term in the amplitude equation) which gives rise to the hexagonal pattern. Therefore, if R_1 is found to be zero, hexagons will not occur, whereas an R_1 different from zero will lead to hexagons.

Let L denote the linear operator of the problem. We then have for the first- and second-order terms

$$L\mathbf{u}_1 - \nabla p_1 = 0, \tag{3.3}$$

$$L\mathbf{u}_2 - \nabla p_2 = \mathbf{u}_1 . \nabla \mathbf{u}_1 - \lambda(z) R_1 w_1 \mathbf{e}. \tag{3.4}$$

Here ∇ denotes the three-dimensional gradient operator and $\mathbf{e}$ a unit vector along the θ axis. $\lambda(z)$ is an arbitrary function of z, being a linear function in the present case. We now make the assumption that the operator (together with the boundary conditions) is self-adjoint, such that

$$\langle \mathbf{u}', L\mathbf{u} \rangle = \langle \mathbf{u}, L\mathbf{u}' \rangle, \tag{3.5}$$

where angle brackets denote the integrated vector product. The condition for (3.4) to have a solution gives

$$\langle \mathbf{u}', \mathbf{u}_1 . \nabla \mathbf{u}_1 \rangle - R_1[\lambda(z) w_1 \theta'] = 0 \tag{3.6}$$

for any solution $\mathbf{u}'$ of (3.3). We have used the fact that the pressure term drops out owing to the condition of incompressibility. Square brackets denote integration over the entire fluid layer. The first term in (3.6) is zero for self-adjoint problems (Schlüter, Lortz & Busse 1965). We therefore conclude that for self-adjoint problems R_1 is zero and the planform is not hexagons.

It may easily be shown that the problem is self-adjoint if the viscosity is a function of z or, in porous convection, the permeability is a function of z. The problem is, however, not self-adjoint in the present case, nor in the transient case nor when the thermal diffusivity varies with z. Therefore, in these problems we do expect a hexagonal pattern, at least for values of R close to R_0.

4. The steady solutions

Equations (2.7)–(2.10) will now be solved by a numerical approach. To simplify the problem we assume that the Prandtl number is infinite, whereby (2.7) becomes linear. As is well known, in Bénard convection this approximation is rather good also for moderate Prandtl numbers. Finite Prandtl number convection will be discussed using an amplitude expansion in § 6.

The velocity may appropriately be written (Chandrasekhar 1961, p. 24; Schülter *et al.* 1965) as

$$\mathbf{v} = (u, v, w) = \boldsymbol{\delta} V = (\partial^2/\partial x \partial z, \partial^2/\partial y \partial z, -\nabla_1^2) V, \tag{4.1}$$

where ∇_1^2 is the horizontal Laplacian. Eliminating the pressure term we obtain from (2.7)–(2.10)

$$\nabla^4 V - \theta = 0, \tag{4.2}$$

$$\nabla^2 \theta - Rz \nabla_1^2 V = \partial\theta/\partial t + \mathbf{v} . \nabla\theta, \tag{4.3}$$

with the boundary conditions

$$\left.\begin{aligned} V = \partial V/\partial z = \partial\theta/\partial z = 0 \quad &\text{at} \quad z = 0, \\ V = \partial V/\partial z = \theta = 0 \quad &\text{at} \quad z = 1. \end{aligned}\right\} \tag{4.4}$$

We consider solutions periodic in the x and y directions. θ may then be expanded in a complete set of Fourier modes, each of them satisfying the boundary conditions

$$\theta = \Sigma B_{pqh} \exp\{i(pkx + qly)\} \cos(h - \tfrac{1}{2})\pi z. \tag{4.5}$$

Here k and l are the components of the wavenumber vector in the x and y directions, respectively. The summation runs through all integers

$$-\infty < p < \infty, \quad -\infty < q < \infty, \quad 1 \leqslant h < \infty.$$

To ensure that (4.5) is real $B_{pqh} = B^*_{-p-qh}$, where the star denotes the complex conjugate. Introducing (4.5) into (4.2) and applying the boundary conditions, we obtain

$$V = \Sigma B_{pqh} \exp\{i(pkx + qly)\} F_h(\kappa, z), \tag{4.6}$$

where $\kappa^2 = (pk)^2 + (ql)^2$. The function $F_h(\kappa, z)$ is given in the appendix.

The unknown coefficients B_{pqh} are determined from (4.3) by applying a Galerkin procedure. Introducing (4.5) and (4.6) into (4.3), multiplying this by $\exp\{-i(rkx + sly)\} \cos(g - \frac{1}{2})\pi z$ and averaging over the fluid layer, we obtain

$$\begin{aligned} \tfrac{1}{2}\dot{B}_{rsg} = & -\tfrac{1}{2}\{((g-\tfrac{1}{2})\pi)^2 + \nu^2\} B_{rsg} + R\nu^2 \sum_h a(h, \nu, g)\, B_{rsh} \\ & + \sum_{\substack{p+t=r \\ q+u=s}} \sum_{h,f} \{(ptk^2 + qul^2)\, b(h, \kappa, f, g) + \kappa^2 c(h, \kappa, f, g)\} B_{pqh} B_{tuf}. \end{aligned} \tag{4.7}$$

Here $\nu^2 = (rk)^2 + (sl)^2$, and the coefficients a, b and c are given in the appendix. Equation (4.7) represents an infinite set of coupled first-order ordinary differential equations.

To solve the problem it is necessary to make some simplifications. According to § 3 the expected planform is hexagons. To first order, hexagons are given by the Fourier modes

$$A_{11} \cos kx \cos ly + A_{02} \cos 2ly, \tag{4.8}$$

$$k^2 + l^2 = 4l^2 = a^2, \quad A_{11} = \pm 2A_{02}. \tag{4.9}$$

It is noted that $A_{11} = 0$ corresponds to two-dimensional rolls, whereas $A_{02} = 0$ corresponds to a rectangular pattern. If the first-order terms are given by (4.8), the higher-order terms excited will be of the form $A_{ij} \cos ikx \cos jly$, where i and j are integers such that $i + j$ is even. We shall seek only steady solutions of this form, which implies that the B_{rsg} are all real and

$$B_{rsg} = B_{-r-sg} = B_{r-sg} = B_{-rsg}.$$

Further, we have found it appropriate to truncate the infinite system of differential equations by neglecting all modes for which $g^2 + \frac{3}{4}r^2 + \frac{1}{4}s^2 > M^2 + 1$. Here the integer M must be chosen such that the solution of the finite system differs by a sufficiently small amount from the solution found by replacing M by $M + 1$. Following Thirlby (1970) we choose the non-dimensional quantity N, defined by

$$N = \Delta T'/\Delta T, \tag{4.10}$$

to represent the solution, where ΔT is the mean temperature difference between the horizontal planes and $\Delta T'$ the temperature difference in the case of pure heat

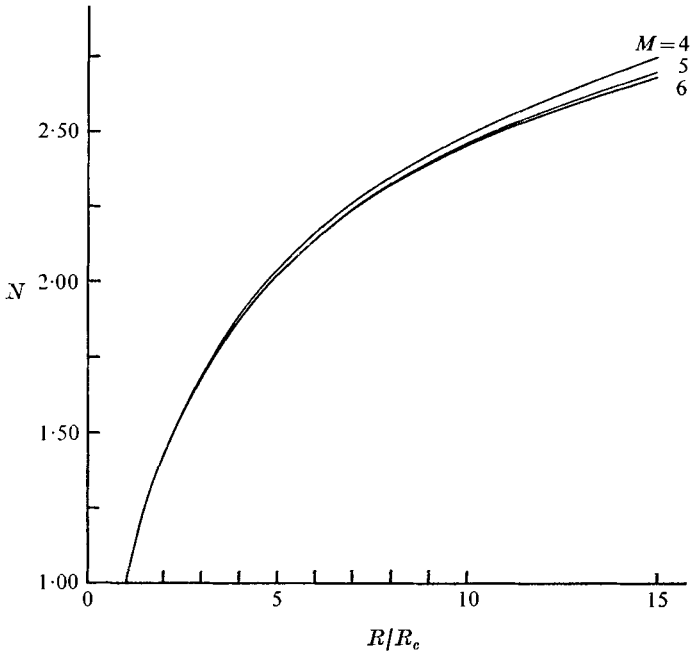

FIGURE 2. The Nusselt number as a function of the Rayleigh number for $M = 4$, 5 and 6. This figure (and figure 3) is based on calculated values for the same Rayleigh numbers as in figure 1. In addition, we have calculated the curves at several points between $R = R_c$ and $R = 3200$.

conduction. We therefore require that $(N_M - N_{M-1})/N_M \equiv \epsilon_M$ be much smaller than unity. N_M for $M = 4$, 5 and 6 is displayed in figure 2. It may be seen that $\epsilon_6 \approx 0{\cdot}007$ for $R/R_c = 15$.

The equations were first solved as an initial-value problem by using a Runge–Kutta method, modified by Kvernvold (1975). Different initial conditions were chosen. For example, in one of the runs A_{02} was put equal to zero, i.e. the initial pattern consisted of rectangular cells. In another run A_{02} (and the higher-order terms) was given a value corresponding to steady two-dimensional rolls whereas A_{11} was chosen very small. In all cases we found that the solution for increasing values of time approaches a hexagonal pattern with downward motion in the centre of each cell.

The subscripts r and s attached to B_{rsg} satisfy an equation of the form $3r^2 + s^2 = 4n$, where n is an integer. The appearance of hexagons for increasing values of time was revealed by the fact that all B_{rsg} with the same n and g approached the same steady value. Some of these coefficients, called B_{ng}, are shown in figure 3 for $a = a_c = 2{\cdot}63$. It is noted that the coefficients B_{01} and B_{11} (and partly B_{02}) tend to dominate for $R/R_c < 15$.

These introductory runs suggested that hexagons are a stable pattern, in contrast to, for example, two-dimensional rolls. We found it desirable, however, to examine the stability of the hexagons more carefully and more broadly. In our runs we considered only motion with a specific wavenumber. We therefore

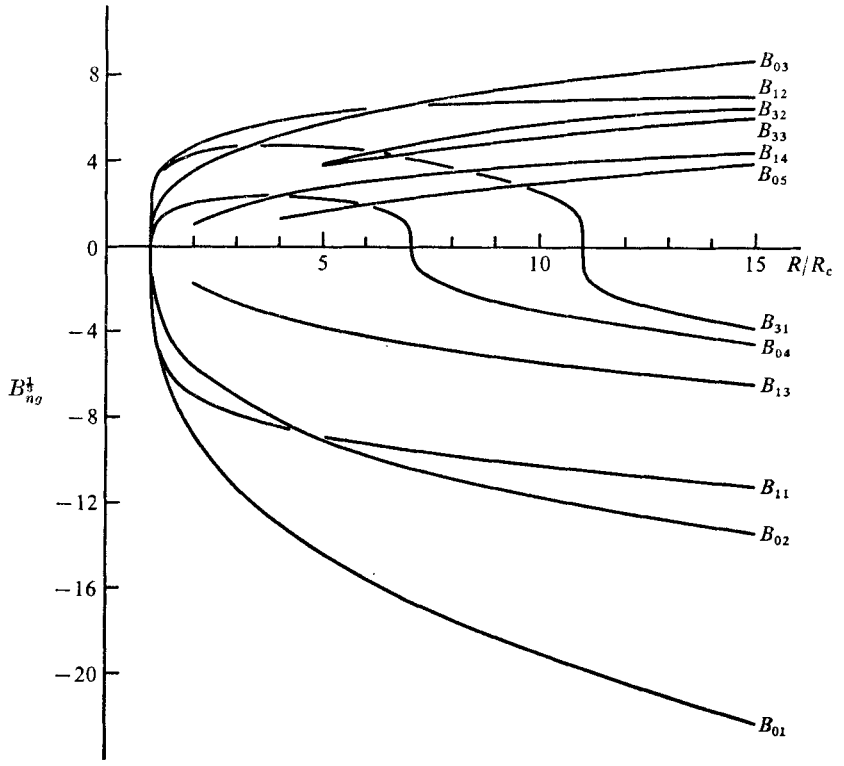

FIGURE 3. Some of the amplitudes *vs.* the Rayleigh number.

wanted to examine the stability behaviour of the hexagons for more general disturbances. We also wanted to consider hexagons of various horizontal wavelengths and for Rayleigh numbers as high as permissible. This led us to seek the steady solutions by a Newton–Raphson method (which converges considerable faster than the Runge–Kutta method) and, as discussed in the next section, to perturb the steady solutions by a rather general disturbance.

The number N defined by (4.10) expresses the heat transport at the upper plane divided by the (virtual) heat transport by pure conduction for the same ΔT. N is therefore a Nusselt number, being unity in the conductive state and larger than unity in the convective regime. Figure 2 shows the relation between the Nusselt number and the Rayleigh number. The same curve is also shown in figure 4 with a logarithmic scale for the R/R_c axis. It is seen that to a good approximation

$$N = C \log (R/R_c) + 1, \tag{4.11}$$

where C is found to be 0·64.

The horizontally averaged temperature (non-dimensional), given by

$$\bar{T} = 0{\cdot}5(1-z^2) + 1/R \sum_g B_{0g} \cos (g - \tfrac{1}{2}) \pi z, \tag{4.12}$$

is shown in figure 5 for various values of R/R_c with $a = a_c$.

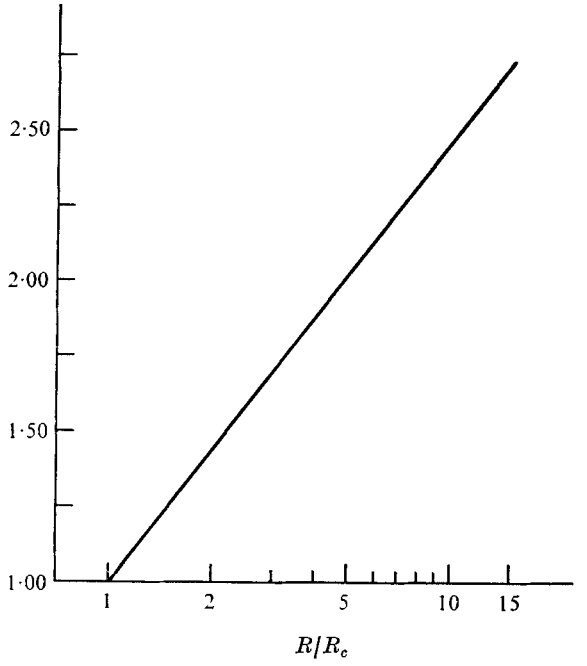

FIGURE 4. The Nusselt number as a function of the Rayleigh number with a logarithmic scale for the R/R_c axis, showing $N = 0{\cdot}64 \log (R/R_c) + 1$.

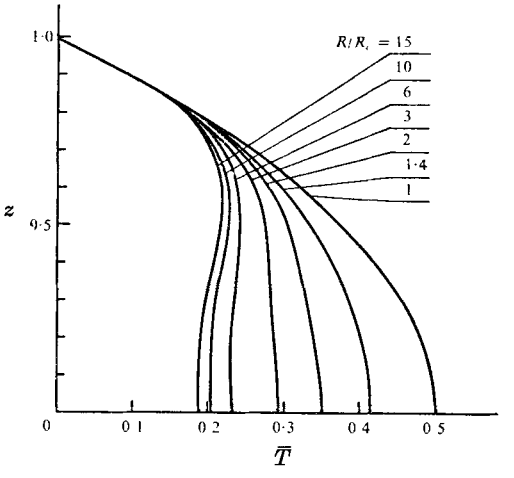

FIGURE 5. The horizontally averaged temperature for different values of R/R_c with $a = a_c$.

5. The stability of the steady solutions

By eliminating the pressure in (2.12) and using the fact that $P = \infty$, we obtain from (2.12)–(2.15)

$$\nabla^4 \tilde{V} - \tilde{\theta} = 0, \tag{5.1}$$

$$\nabla^2 \tilde{\theta} - Rz\nabla_1^2 \tilde{V} = \sigma\tilde{\theta} + \mathbf{v}.\nabla\tilde{\theta} + \tilde{\mathbf{v}}.\nabla\theta, \tag{5.2}$$

where $$\tilde{\mathbf{v}} = (\tilde{u}, \tilde{v}, \tilde{w}) = \boldsymbol{\delta}\tilde{V} = (\partial^2/\partial x\,\partial z, \partial^2/\partial y\,\partial z, -\nabla_1^2)\,\tilde{V}. \tag{5.3}$$

The boundary conditions are

$$\left.\begin{aligned} \tilde{V} = \partial\tilde{V}/\partial z = \partial\tilde{\theta}/\partial z = 0 \quad &\text{at} \quad z = 0, \\ \tilde{V} = \partial\tilde{V}/\partial z = \tilde{\theta} = 0 \quad &\text{at} \quad z = 1. \end{aligned}\right\} \tag{5.4}$$

Introducing in (5.2) the steady solution corresponding to hexagons, a characteristic solution satisfying the boundary conditions may be written as

$$\tilde{\theta} = \exp\{i(\epsilon kx + \delta ly)\} \Sigma \tilde{B}_{pqh} \exp\{i(pkx + qly)\} \cos(h - \tfrac{1}{2})\pi z, \tag{5.5}$$

$$\tilde{V} = \exp\{i(\epsilon kx + \delta ly)\} \Sigma \tilde{B}_{pqh} \exp\{i(pkx + qly)\}\, F_h(\tilde{\kappa}, z), \tag{5.6}$$

where $\tilde{\kappa}^2 = (p+\epsilon)^2 k^2 + (q+\delta)^2 l^2$ and $F_h(\kappa, z)$ is given in the appendix. ϵ and δ are arbitrary constants. When ϵ and δ are given all relevant values, (5.5) and (5.6) represent an arbitrary disturbance. It may be shown that in our problem (i.e. for a hexagonal pattern) it suffices to choose $0 \leqslant \delta \leqslant 1$ and $0 \leqslant \epsilon \leqslant \frac{1}{3}\delta$.

By multiplying (5.2) by $\exp\{-i(\epsilon kx + \delta ly)\} \exp\{-i(rkx + sly)\} \cos(g - \frac{1}{2})\pi z$ and taking the average over the fluid layer, we obtain an infinite set of linear homogeneous equations determining the coefficients $\tilde{B}_{rsg}$. As in the preceding section we neglect modes for which $g^2 + \frac{3}{4}r^2 + \frac{1}{4}s^2 > M^2 + 1$. The stability problem is now reduced to finding σ from the eigenvalue problem for the finite system of equations.

The results of the computations are displayed in figure 1. We have here set $M = 4$ for $R_c < R < 10R_c$, $M = 5$ for $8R_c < R < 18R_c$ and $M = 6$ for

$$12R_c < R < 30R_c.$$

In the overlaps between these intervals we get, as indicated in the figure, a check on the accuracy of the computations. The curves in the figure are drawn as solid lines up to $R = 15R_c$, where $M = 5$ and $M = 6$ give approximately the same result. The curves are dashed from $15R_c$ up to $20R_c$ since there is some discrepancy between the curves for $M = 5$ and $M = 6$. We found also that the curve had a similar appearance in the region $20R_c < R < 30R_c$. It is noted that the stable region for hexagons is rather narrow and centred about $a = a_c$.

In the computations above we have assumed that σ is real. This is a simplifying approximation which is usually believed to be valid for infinite Prandtl number, and therefore no shearing instability occurs (for ordinary Bénard convection, see Busse 1972).

6. The amplitude expansion

When we started this problem, we expected to find a finite region of subcritical instability. An amplitude expansion would then be of little interest since the validity of such an expansion most likely would be limited to the subcritical branch corresponding to unstable hexagons. However, the numerical computations revealed that the subcritical region, if it exists, must be of rather small extent. In that case an amplitude expansion may be of interest, partly as a means to examine the possible subcritical region and partly to find the motion for small supercritical Rayleigh numbers in fluids with finite Prandtl number.

Intending to take into account terms up to the third order only, we write

$$R - R_0 = \Delta R = R_1 + R_2 + \ldots, \tag{6.1}$$

$$\mathbf{v} = \mathbf{v}_1 + \mathbf{v}_2 + \ldots, \quad \theta = \theta_1 + \theta_2 + \ldots, \quad p = p_1 + p_2 + \ldots, \tag{6.2)–(6.4}$$

where, as in § 3, R_1 denotes the first approximation, $R_1 + R_2$ the second approximation, etc. and similarly for the other quantities. According to (2.7) and (2.9), the first-order equations are

$$\nabla^2 \mathbf{v}_1 + \theta_1 \mathbf{k} - \nabla p_1 = 0, \tag{6.5}$$

$$\nabla^2 \theta_1 + R_0 z w_1 = 0. \tag{6.6}$$

The solution of (6.5) and (6.6) satisfying (2.8) and the boundary conditions (2.10) may be written as

$$\theta_1 = \sum_{\substack{n=-L \\ n \neq 0}}^{L} C_n w_n g(z), \quad w_n = \exp(i\mathbf{k}_n . \mathbf{r}), \quad \mathbf{k}_n = -\mathbf{k}_{-n}, \quad C_n = C^*_{-n}, \tag{6.7}$$

$$\mathbf{v}_1 = \boldsymbol{\delta} \sum_{\substack{n=-L \\ n \neq 0}}^{L} C_n w_n f(z), \tag{6.8}$$

where $g(z)$ and $f(z)$ are given in the appendix.

The adjoint problem to (6.5), (6.6), (2.8) and (2.10) is

$$\nabla^2 \hat{\mathbf{v}} + R_0 z \hat{\theta} \mathbf{k} - \nabla \hat{p} = 0, \tag{6.9}$$

$$\nabla^2 \hat{\theta} + \hat{w} = 0, \quad \nabla . \hat{\mathbf{v}} = 0, \tag{6.10), (6.11}$$

with the boundary conditions

$$\left.\begin{aligned} \hat{\mathbf{v}} = \partial \hat{\theta}/\partial z = 0 \quad &\text{at} \quad z = 0, \\ \hat{\mathbf{v}} = \hat{\theta} = 0 \quad &\text{at} \quad z = 1. \end{aligned}\right\} \tag{6.12}$$

An arbitrary solution of (6.9)–(6.11) satisfying (6.12) may be written as

$$\hat{\theta}_N = \hat{w}_N \hat{g}(z), \quad \hat{w}_N = \exp(-i\mathbf{k}_N . \mathbf{r}), \tag{6.13}$$

$$\hat{\mathbf{v}}_N = \boldsymbol{\delta}(\hat{w}_N \hat{f}(z)), \tag{6.14}$$

where $\hat{f}(z)$ and $\hat{g}(z)$ are given in the appendix.

Assuming that $\partial/\partial t$ is of second order, the second-order terms are given by

$$\nabla^2 \mathbf{v}_2 + \theta_2 \mathbf{k} - \nabla p_2 = P^{-1} \mathbf{v}_1 . \nabla \mathbf{v}_1, \tag{6.15}$$

$$\nabla^2 \theta_2 + R_0 z w_2 = \mathbf{v}_1 . \nabla \theta_1 - R_1 z w_1. \tag{6.16}$$

Correspondingly, for the third-order terms

$$\nabla^2 \mathbf{v}_3 + \theta_3 \mathbf{k} - \nabla p_3 = P^{-1}(\mathbf{v}_1 . \nabla \mathbf{v}_2 + \mathbf{v}_2 . \nabla \mathbf{v}_1 + \partial \mathbf{v}_1/\partial t), \tag{6.17}$$

$$\nabla^2 \theta_3 + R_0 z w_3 = \mathbf{v}_1 . \nabla \theta_2 + \mathbf{v}_2 . \nabla \theta_1 + \partial \theta_1/\partial t - R_1 z w_2 - R_2 z w_1. \tag{6.18}$$

The solution of the second-order equations is given in the appendix.

The solvability conditions for (6.15) and (6.16) and for (6.17) and (6.18) determine R_1 and R_2, respectively:

$$R_1[\hat{\theta}_N z w_1] = [\hat{\theta}_N \mathbf{v}_1 . \nabla\theta_1] + P^{-1}[\hat{\mathbf{v}}_N . (\mathbf{v}_1 . \nabla \mathbf{v}_1)], \tag{6.19}$$

$$R_2[\hat{\theta}_N z w_1] = [\hat{\theta}_N(\mathbf{v}_1 . \nabla\theta_2 + \mathbf{v}_2 . \nabla\theta_1 + \partial\theta_1/\partial t - R_1 z w_2)] + P^{-1}[\hat{\mathbf{v}}_N . (\mathbf{v}_1 . \nabla \mathbf{v}_2 + \mathbf{v}_2 . \nabla \mathbf{v}_1 + \partial \mathbf{v}_1/\partial t)], \tag{6.20}$$

where square brackets denote integration over the fluid layer.

We shall restrict the investigation to the case when L in (6.7) and (6.8) is 3 and the wavenumber vectors $\mathbf{k}_1$, $\mathbf{k}_2$ and $\mathbf{k}_3$ are inclined at 120° to each other. This system of modes contains the system (4.8) discussed in §4, and has, besides the hexagon solution, several other steady solutions. After some computations it is found by introducing the expressions for R_1 and R_2 into (6.1) that

$$M\dot{C}_N = \Delta R C_N - A C^*_{N+1} C^*_{N-1} - \{P_1 C_N C^*_N + P_2(C_{N+1} C^*_{N+1} + C_{N-1} C^*_{N-1})\} C_N. \tag{6.21}$$

Here $N = 1$, 2 or 3 and $C_0 = C_3$ and $C_4 = C_1$. The other quantities are found to be (see appendix)

$$\left.\begin{aligned} M &= 255 + 73P^{-1}, \quad A = -14{\cdot}71 + 3{\cdot}687P^{-1}, \\ P_1 &= 8{\cdot}639 - 0{\cdot}0284P^{-1} + 0{\cdot}0373P^{-2}, \\ P_2 &= 10{\cdot}40 + 0{\cdot}4707P^{-1} + 0{\cdot}2088P^{-1}. \end{aligned}\right\} \tag{6.22}$$

The system of equations (6.21) is formally identical to the system of six real equations in the ordinary Bénard problem discussed by Segel (1965, see also Busse 1962). Segel found that for supercritical Rayleigh numbers the system has three different types of possible equilibrium solution: (*a*) hexagonal cells, (*b*) two-dimensional roll cells, (*c*) a special closed cell labelled 'V' in Segel & Stuart (1962).

The equations also permit subcritical steady solutions in form of hexagons. In Bénard convection (*c*) is shown to be unstable. This is also found to be true in the present problem (since the quantity Q, defined below, is positive). We then formally end up with the same type of stable solutions as Segel. With essentially his notation we find that hexagons are the only stable planform in the range $-a'^2/4T < \Delta R < a'^2 R_1/Q^2$, both hexagons and two-dimensional rolls are stable for $a'^2 R_1/Q^2 < \Delta R < a'^2(4R' + R_1)/Q^2$ whereas two-dimensional rolls are the only stable planform for $\Delta R > a'^2(4R' + R_1)/Q^2$. In the present problem

$$\left.\begin{aligned} a' &= A, \quad R' = \tfrac{1}{4}(P_1 + P_2), \quad R_1 = P_1, \\ Q &= P_2 - P_1, \quad T = 2P_2 + P_1. \end{aligned}\right\} \tag{6.23}$$

As shown in figure 6 the subcritical range is rather small. It may be noted from figure 7 that the interval containing stable hexagons depends noticeably on the Prandtl number. This may also be seen from table 1. We have checked the result in table 1 for the subcritical Rayleigh number in case of infinite Prandtl number by very detailed numerical computations, applying a Galerkin method. We found no steady solution for $R = 2770{\cdot}3$ whereas a steady solution was obtained for $R = 2770{\cdot}5$. This is in very good agreement with the amplitude expansion, which gives the subcritical Rayleigh number 2770·43 (where we have used the more exact value $-1{\cdot}84$ for ΔR_{-1}).

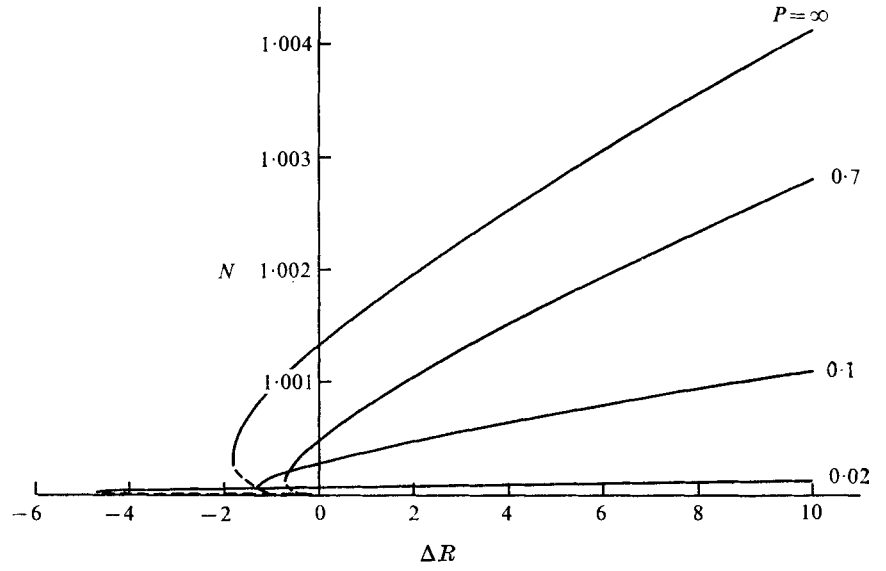

FIGURE 6. The Nusselt number as a function of the Rayleigh number close to R_c for different values of P. – – –, unstable motion; ——, stable motion.

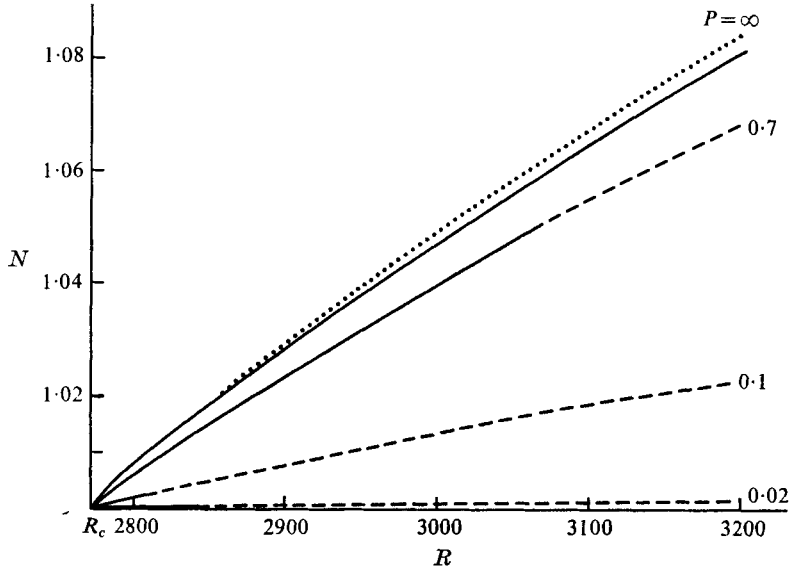

FIGURE 7. The Nusselt number as a function of the Rayleigh number for different values of P. – – –, unstable motion; ——, stable motion; ····, numerical calculations.

P	ΔR_{-1}	ΔR_1	ΔR_2
∞	−1·8	600	2000
5·5	−1·7	500	1600
0·7	−0·7	90	300
0·02	−4·7	10	70

TABLE 1. Hexagons are stable for $\Delta R_{-1} < \Delta R < \Delta R_2$ and two-dimensional rolls are stable for $\Delta R > \Delta R_1$

We note that for infinite Prandtl number hexagons occur for Rayleigh numbers up to about $1{\cdot}7R_c$ whereas the numerical calculations gave hexagons up to at least $15R_c$. This discrepancy shows that the amplitude expansion containing only three terms is only reliable rather close to the critical Rayleigh number. On the other hand, it may be seen from figure 7 that the amplitude expansion gives fair agreement for the Nusselt number. This only confirms what is well known, that a useful approximation to the Nusselt number may be obtained by rather crude methods.

From (6.21), the sign of the circulation in the hexagons is determined by the sign of A. It is found that the sign is negative for large and moderate Prandtl numbers, which gives down-hexagons. However, for values of P less than 0·25 the coefficient changes sign and we obtain up-hexagons. For values of the Prandtl number close to 0·25 the planform will be two-dimensional rolls.

7. Summary and conclusion

The main result of the paper is demonstrated in figure 1, where it is shown that hexagons are stable at least up to 15 times R_c. There is nothing in the computations which indicates that hexagons become unstable for higher Rayleigh numbers. The computations reveal that hexagons are formed even if the initial motion has a quite different pattern. The numerical calculations are confined to infinite Prandtl number, which is generally believed also to cover the case of moderate Prandtl numbers.

To examine more closely the possibilities for subcritical convection and also to study the motion for various Prandtl numbers, we applied an amplitude expansion, retaining only the three first terms. This expansion is only valid close to R_c, where we obtain satisfactory agreement with the numerical calculations. For higher Rayleigh numbers the amplitude expansion indicates that two-dimensional rolls become the only stable mode. The expansion is, however, not valid for these Rayleigh numbers, at least for large Prandtl numbers. We note that the Rayleigh number region corresponding to hexagons found from the amplitude expansion is much too small. This is probably also the case for ordinary Bénard convection (Hoard, Robertson & Acrivos 1970).

For high and moderate values of the Prandtl number we find that the hexagons are down-hexagons, i.e. with descending motion at the cell centres. For Prandtl numbers less than 0·25 we obtain stable hexagons with ascending motion at the cell centres.

In §3 we have examined the horizontal planform in the case when the coefficients in the differential equations depend on z. It is shown that a necessary condition for obtaining hexagons is that the linear problem is not self-adjoint.

Our results are in accordance with the available observational data as far as the type of planform is concerned (Tritton & Zarraga 1967; Schwiderski & Schwab 1971). The experiments are, however, confined to Rayleigh numbers larger than $4R_c$, there being no observations for Rayleigh numbers close to R_c. According to the theory the observed diameter of the cells should be close to the critical value. This is not found in the experiments, where the horizontal length scale increases

markedly with the Rayleigh number. According to Schwiderski & Schwab, the explanation for this discrepancy is most likely that the heating due to the electric current is rather strongly dependent on the temperature, and therefore not uniform in space. Indeed, by doubling the depth of the fluid layer in their experiments (whereby the difference in temperature between the horizontal planes was lowered by a factor of eight) they found that the increase in the diameter was effectively reduced.

The results of our work may also be compared with earlier theoretical work by Roberts (1967) and Thirlby (1970). There is agreement as to the sign of the circulation in the cells (when $P > 0{\cdot}25$) and the type of planform for moderate values of R. Roberts finds, however, that hexagons are not stable for small supercritical Rayleigh numbers. For water R must be larger than about $3R_c$ in order that hexagons are stable. Thirlby finds that a rectangular pattern is stable for Rayleigh numbers less than about $5R_c$ and that hexagons are stable above this value. In favour of our result is the fact that we obtain the same answer for small supercritical Rayleigh numbers by both our methods. Another point is that it seems reasonable that a subcritical region consisting of hexagons exists in the present case. By continuity arguments we then expect hexagons also for small supercritical Rayleigh numbers.

Appendix

From (4.2) and (4.4)–(4.6) we obtain

$$(d^2/dz^2-\kappa^2)^2 F_h(\kappa,z) = \cos(h-\tfrac{1}{2})\pi z, \tag{A 1}$$

with the boundary conditions

$$F_h(\kappa,z) = F_h'(\kappa,z) = 0 \quad \text{at} \quad z = 0, 1. \tag{A 2}$$

The solution is

$$F_h(\kappa,z) = A_h(\kappa)\cos(h-\tfrac{1}{2})\pi z + C_h^{(1)}(\kappa)\cosh\kappa z + C_h^{(2)}(\kappa) z\cosh\kappa z + C_h^{(3)}(\kappa)\sinh z + C_h^{(4)}(\kappa) z\sinh\kappa z, \tag{A 3}$$

where

$$A_h(\kappa) = ((h-\tfrac{1}{2})^2\pi^2+\kappa^2)^{-2}, \tag{A 4a}$$

$$C_h^{(1)}(\kappa) = -A_h(\kappa), \tag{A 4b}$$

$$C_h^{(2)}(\kappa) = A_h(\kappa)(\kappa^2+\kappa\cosh\kappa\sinh\kappa+(-1)^h(h-\tfrac{1}{2})\pi\kappa\sinh\kappa)/(\kappa^2-\sinh^2\kappa), \tag{A 4c}$$

$$C_h^{(3)}(\kappa) = -C_h^{(2)}(\kappa)/\kappa, \tag{A 4d}$$

$$C_h^{(4)}(\kappa) = (A_h(\kappa)\cosh\kappa + C_h^{(3)}(\kappa)(\kappa\cosh\kappa-\sinh\kappa))/\sinh\kappa. \tag{A 4e}$$

The coefficients a, b and c in (4.7) are defined by

$$a(h,\nu,g) = \int_0^1 z F_h(\nu,z)\cos(g-\tfrac{1}{2})\pi z\,dz, \tag{A 5a}$$

$$b(h,\kappa,f,g) = \int_0^1 F_h'(\kappa,z)\cos(f-\tfrac{1}{2})\pi z\cos(g-\tfrac{1}{2})\pi z\,dz, \tag{A 5b}$$

$$c(h,\kappa,f,g) = (f-\tfrac{1}{2})\pi\int_0^1 F_h(\kappa,z)\sin(f-\tfrac{1}{2})\pi z\cos(g-\tfrac{1}{2})\pi z\,dz. \tag{A 5c}$$

		$F_0(\beta, z) \times 10^3$			$F_p(\beta, z) \times 10^3$			
$f(z)$	$\hat{g}(z)$	$\beta = -\frac{1}{2}$	$\beta = \frac{1}{2}$	$\beta = 1$	$\beta = -\frac{1}{2}$	$\beta = \frac{1}{2}$	$\beta = 1$	$G_0(-1, z)$
0	1·000	0	0	0	0	0	0	−0·1750
0	0	0	0	0	0	0	0	0
−0·4263	3·458	0·2558	0·2692	0·2411	0·6557	−0·1089	−0·1088	0
1·0000	0	−0·0971	−0·8862	−0·9690	−0·1607	0·4066	0·5129	1·497
−0·9304	−19·68	−0·2715	1·467	1·863	1·650	−0·3569	−0·5029	−2·634
0·6917	24·75	−0·0672	−1·839	−2·681	4·947	0·8436	−1·610	5·067

TABLE 2. The first six coefficients in the power series for $f(z)$, $\hat{g}(z)$, $F_0(\beta, z)$, $F_p(\beta, z)$ and $G_0(-1, z)$

By introducing the expressions (6.7) and (6.8) into (6.5) and (6.6) and eliminating the pressure, we obtain the equations for f and g:

$$(d^2/dz^2 - a^2)^3 f + R_0 z f = 0, \qquad (d^2/dz^2 - a^2) f - g = 0, \tag{A 6}$$

with the boundary conditions

$$f = f' = g' = 0 \quad \text{at} \quad z = 0, \qquad f = f' = g = 0 \quad \text{at} \quad z = 1. \tag{A 7}$$

f and g may conveniently be written in the form (Sparrow *et al.* 1964)

$$f = \sum_{n=0}^{\infty} A_n z^n, \quad g = \sum_{n=0}^{\infty} B_n z^n. \tag{A 8}$$

$A_0, A_1, \ldots, A_5$ are given in table 2 for $a = a_c$. The other coefficients A_n and B_n are then easily obtained from (A 6).

In the same manner we obtain the equations for $\hat{f}$ and $\hat{g}$ from (6.9)–(6.14):

$$(d^2/dz^2 - a^2)^3 \hat{g} + R_0 z \hat{g} = 0, \quad (d^2/dz^2 - a^2) \hat{g} + a^2 f = 0, \tag{A 9}$$

with the boundary conditions

$$\hat{f} = \hat{f}' = \hat{g}' = 0 \quad \text{at} \quad z = 0, \qquad \hat{f} = \hat{f}' = \hat{g} = 0 \quad \text{at} \quad z = 1. \tag{A 10}$$

The first six coefficients in the power-series expansion for $\hat{g}$ are given in table 2.

Finally, the solution of (6.15) and (6.16) may be written as

$$\left.\begin{aligned} \theta_2 &= \sum_{n,m} a^2 C_n C_m w_n w_m G(\beta, z), \quad \beta = \phi_{nm} = \mathbf{k}_n . \mathbf{k}_m / a^2, \\ \mathbf{v}_2 &= \boldsymbol{\delta} \sum_{n,m} a^2 C_n C_m w_n w_m F(\beta, z). \end{aligned}\right\} \tag{A 11}$$

Here $$G(\beta, z) = G_0(\beta, z) + P^{-1} G_p(\beta, z), \quad F(\beta, z) = F_0(\beta, z) + P^{-1} F_p(\beta, z). \tag{A 12}$$

Introducing (A 11) into (6.15) and (6.16) gives

$$\begin{aligned} \{d^2/dz^2 - 2a^2(1+\beta)\}^3 F(\beta, z) + R_0 2a^2(1+\beta) z F(\beta, z) &= f g' - \beta f' g - \tfrac{1}{2} I(\beta) A z f \\ &+ P^{-1}\{\tfrac{1}{2}(f^{(5)} f + (\tfrac{3}{2} - \beta) f^{(4)} f' + (2 - 3\beta) f''' f'' - a^2(1-\beta)(f''' f + 3 f'' f')) \\ &- a^2(1+\beta)(f''' f + (1-2\beta) f'' f' - 2a^2(1-\beta) f' f)\}, \end{aligned} \tag{A 13a}$$

$$\{d^2/dz^2 - 2a^2(1+\beta)^2\} F(\beta, z) - G(\beta, z) = (2P)^{-1}\{f''' f - (1-2\beta) f'' f' - 2a^2(1-\beta) f' f\}, \tag{A 13b}$$

with the boundary conditions

$$F = F' = G' = 0 \quad \text{at} \quad z = 0, \qquad F = F' = G = 0 \quad \text{at} \quad z = 1. \quad \text{(A 14)}$$

Here A is given by (6.22), $I(\beta) = 1$ for $\beta = -\frac{1}{2}$ and $I(\beta) = 0$ for $\beta \neq -\frac{1}{2}$. The first six coefficients in the power-series expansions for $F(\beta, z)$ and $G_0(-1, z)$ are given in table 2. $G_0(-1, z)$ is given by the non-harmonic part of (6.16).

In order to calculate the coefficients in (6.21) we need the following expressions for the terms in (6.19) and (6.20):

$$[\hat{\theta}_N z w_1] = a^2 C_N \int_0^1 z f \hat{g}\, dz,$$

$$\left[\hat{\theta}_N \frac{\partial}{\partial t}\theta_1\right] = \dot{C}_N \int_0^1 g \hat{g}\, dz,$$

$$\left[\hat{\mathbf{v}}_N \cdot \frac{\partial}{\partial t}\mathbf{v}_1\right] = a^2 \dot{C}_N \int_0^1 (f'\hat{f}' + a^2 f\hat{f})\, dz,$$

$$[\hat{\theta}_N z w_2] = 2a^4 \sum_{n,m} C_n C_m (1 + \phi_{nm}) \int_0^1 z F(\phi_{nm}, z)\, \hat{g}\, dz,$$

$$[\hat{\theta}_N \mathbf{v}_1 \cdot \nabla \theta_1] = a^2 \sum_{n,m} C_n C_m \int_0^1 (fg' - \phi_{nm} f' g)\, \hat{g}\, dz,$$

$$[\hat{\theta}_N \mathbf{v}_1 \cdot \nabla \mathbf{v}_1] = a^4 \sum_{n,m} C_n C_m \int_0^1 \{\phi_{nm}(ff'' - \phi_{nm} f'^2)\hat{f}' + a^2(1 - \phi_{nm}) f' f \hat{f}\}\, dz,$$

where the sums run through all n and m such that $\mathbf{k}_n + \mathbf{k}_m = \mathbf{k}_N$,

$$[\hat{\theta}_N \mathbf{v}_1 \cdot \nabla \theta_2] = a^4 \sum_{l,n,m} C_l C_n C_m \int_0^1 \{fG(\phi_{nm}, z) - (\phi_{ln} + \phi_{lm}) f' G(\phi_{nm}, z)\}\, \hat{g}\, dz,$$

$$[\hat{\theta}_N \hat{\mathbf{v}}_2 \cdot \nabla \theta_1] = a^4 \sum_{l,n,m} C_l C_n C_m \int_0^1 \{2(1 + \phi_{nm}) g' F(\phi_{nm}, z) - (\phi_{ln} + \phi_{lm}) g F'(\phi_{nm}, z)\}\, \hat{g}\, dz,$$

$$[\hat{\mathbf{v}}_N \cdot (\mathbf{v}_1 \cdot \nabla \mathbf{v}_2)] = a^6 \sum_{l,n,m} C_l C_n C_m \int_0^1 \{(\phi_{Nn} + \phi_{Nm})[fF''(\phi_{nm}, z) - (\phi_{ln} + \phi_{lm}) f' F'(\phi_{nm}, z)]\hat{f}' + 2a^2(1 + \phi_{nm})[fF'(\phi_{nm}, z) - (\phi_{ln} + \phi_{lm}) f' F(\phi_{nm}, z)]\hat{f}\}\, dz,$$

$$[\hat{\mathbf{v}}_N \cdot (\mathbf{v}_2 \cdot \nabla \mathbf{v}_1)] = a^6 \sum_{l,n,m} C_l C_n C_m \int_0^1 \{\phi_{Nl}[2(1 + \phi_{nm}) f'' F(\phi_{nm}, z) - (\phi_{ln} + \phi_{lm}) f' F'(\phi_{nm}, z)]\hat{f}' + a^2[2(1 + \phi_{nm}) f' F(\phi_{nm}, z) - (\phi_{ln} + \phi_{lm}) f F'(\phi_{nm}, z)]\hat{f}\}\, dz,$$

where the sums run through all l, n and m such that $\mathbf{k}_1 + \mathbf{k}_n + \mathbf{k}_m = \mathbf{k}_N$.

REFERENCES

Busse, F. H. 1962 Dissertion, University of Munich.

Busse, F. H. 1972 *J. Fluid Mech.* **52**, 97.

Chandrasekhar, S. 1961 *Hydrodynamic and Hydromagnetic Stability*. Oxford: Clarendon Press.

HERRING, J. R. 1963 *J. Atmos. Sci.* **20**, 325.

HERRING, J. R. 1964 *J. Atmos. Sci.* **21**, 277.

HOARD, C. O., ROBERTSON, C. R. & ACRIVOS, A. 1970 *Int. J. Heat Mass Transfer*, **13**, 849.

KRISHNAMURTI, R. 1968*a* *J. Fluid Mech.* **33**, 445.

KRISHNAMURTI, R. 1968*b* *J. Fluid Mech.* **33**, 457.

KULACKI, F. A. & GOLDSTEIN, R. J. 1972 *J. Fluid Mech.* **55**, 271.

KVERNVOLD, O. 1975 *Inst. Math., Univ. Oslo, Preprint Ser.* no. 1.

MCKENZIE, D. P., ROBERTS, J. M. & WEISS, N. O. 1974 *J. Fluid Mech.* **62**, 465.

PALM, E. 1960 *J. Fluid Mech.* **8**, 183.

PALM, E. 1975 *Ann. Rev. Fluid Mech.* **7**, 39.

PALM, E., ELLINGSEN, T. & GJEVIK, B. 1967 *J. Fluid Mech.* **30**, 651.

ROBERTS, P. H. 1967 *J. Fluid Mech.* **30**, 33.

SCHLÜTER, A., LORTZ, D. & BUSSE, F. H. 1965 *J. Fluid Mech.* **23**, 129.

SCHWIDERSKI, E. W. & SCHWAB, H. J. A. 1971 *J. Fluid Mech.* **48**, 703.

SEGEL, L. A. 1965 *J. Fluid Mech.* **21**, 359.

SEGEL, L. A. & STUART, J. T. 1962 *J. Fluid Mech.* **13**, 289.

SPARROW, E. M., GOLDSTEIN, R. J. & JONSSON, V. K. 1964 *J. Fluid Mech.* **18**, 513.

THIRLBY, R. 1970 *J. Fluid Mech.* **44**, 673.

TRITTON, D. J. & ZARRAGA, M. N. 1967 *J. Fluid Mech.* **30**, 21.

WHITEHEAD, J. A. & CHEN, M. M. 1970 *J. Fluid Mech.* **40**, 549.